

# *Salmonella* Rapidly Regulates Membrane Permeability To Survive Oxidative Stress

Joris van der Heijden,<sup>a,b</sup> Lisa A. Reynolds,<sup>a</sup> Wanyin Deng,<sup>a</sup> Allan Mills,<sup>c</sup> Roland Scholz,<sup>a</sup> Koshi Imami,<sup>d</sup> Leonard J. Foster,<sup>d</sup> Franck Duong,<sup>c</sup> B. Brett Finlay<sup>a,b,c</sup>

Michael Smith Laboratories, University of British Columbia, Vancouver, British Columbia, Canada<sup>a</sup>; Department of Microbiology and Immunology, University of British Columbia, Vancouver, British Columbia, Canada<sup>b</sup>; Department of Biochemistry and Molecular Biology, University of British Columbia, Vancouver, British Columbia, Canada<sup>c</sup>; Center for High-Throughput Biology, University of British Columbia, Vancouver, British Columbia, Canada<sup>d</sup>

**ABSTRACT** The outer membrane (OM) of Gram-negative bacteria provides protection against toxic molecules, including reactive oxygen species (ROS). Decreased OM permeability can promote bacterial survival under harsh circumstances and protects against antibiotics. To better understand the regulation of OM permeability, we studied the real-time influx of hydrogen peroxide in *Salmonella* bacteria and discovered two novel mechanisms by which they rapidly control OM permeability. We found that pores in two major OM proteins, OmpA and OmpC, could be rapidly opened or closed when oxidative stress is encountered and that the underlying mechanisms rely on the formation of disulfide bonds in the periplasmic domain of OmpA and TrxA, respectively. Additionally, we found that a *Salmonella* mutant showing increased OM permeability was killed more effectively by treatment with antibiotics. Together, these results demonstrate that Gram-negative bacteria regulate the influx of ROS for defense against oxidative stress and reveal novel targets that can be therapeutically targeted to increase bacterial killing by conventional antibiotics.

**IMPORTANCE** Pathogenic bacteria have evolved ways to circumvent inflammatory immune responses. A decrease in bacterial outer membrane permeability during infection helps protect bacteria from toxic molecules produced by the host immune system and allows for effective colonization of the host. In this report, we reveal molecular mechanisms that rapidly alter outer membrane pores and their permeability in response to hydrogen peroxide and oxidative stress. These mechanisms are the first examples of pores that are rapidly opened or closed in response to reactive oxygen species. Moreover, one of these mechanisms can be targeted to artificially increase membrane permeability and thereby increase bacterial killing by the antibiotic cefotaxime during *in vitro* experiments and in a mouse model of infection. We envision that a better understanding of the regulation of membrane permeability will lead to new targets and treatment options for multidrug-resistant infections.

Received 14 July 2016 Accepted 18 July 2016 Published 9 August 2016

**Citation** van der Heijden J, Reynolds LA, Deng W, Mills A, Scholz R, Imami K, Foster LJ, Duong F, Finlay BB. 2016. *Salmonella* rapidly regulates membrane permeability to survive oxidative stress. mBio 7(4):e01238-16. doi:10.1128/mBio.01238-16.

**Editor** Samuel I. Miller, University of Washington

**Copyright** © 2016 van der Heijden et al. This is an open-access article distributed under the terms of the [Creative Commons Attribution 4.0 International license](https://creativecommons.org/licenses/by/4.0/).

Address correspondence to B. Brett Finlay, [bfm@interchange.ubc.ca](mailto:bfm@interchange.ubc.ca).

This article is a direct contribution from a Fellow of the American Academy of Microbiology. External solicited reviewers: Dirk Bumann, Biozentrum; Wolf Hardt, Institute of Microbiology, ETH Zurich.

During infection with bacterial pathogens, the immune response of healthy individuals generates antimicrobial reactive oxygen species (ROS) to kill invading bacteria. The outer membrane (OM) of Gram-negative bacterial pathogens provides protection from a variety of environmental stresses, including ROS (1). ROS can permeate through the bacterial membrane to cause damage to bacterial proteins, DNA, and other intrabacterial molecules (2, 3). However, very little is known about if or how bacteria regulate the influx of ROS. The influx of antibiotics has been more extensively studied (1, 4). Typically, hydrophobic compounds diffuse through the OM while hydrophilic molecules permeate into bacteria predominantly through pores in OM proteins (OMPs) (1). Since many antibiotics enter through OM pores, accurate regulation of OMP expression lies at the core of antibiotic resistance, which is clearly illustrated by a decreased OM permeability in a majority of the multidrug-resistant bacteria

isolated from patients in clinics (5, 6). Recent studies have revealed that there are subsets of pathogens in different tissue microenvironments with disparate outcomes of antibiotic treatment (7). Certain subsets include nonreplicating antibiotic-tolerant cells that limit OM permeability and often reinitiate a full-blown infection after antibiotic treatment is completed (1, 8–13). Because of this, it has been suggested that targeting the OM to increase permeability is an underexploited strategy to increase antibiotic efficacy (14). Recently, we described an analytical method that relies on redox-sensitive green fluorescent protein (GFP), called roGFP2, to measure redox changes directly inside bacteria, enabling us to measure the real-time influx of ROS (15, 16). In this study, we used this system to accurately measure the real-time influx of H<sub>2</sub>O<sub>2</sub> into living *Salmonella enterica* serovar Typhimurium bacteria during exposure to ROS and identified regulatory mechanisms that alter OM permeability and ROS sensitivity.

## RESULTS

**Pores in OMPs facilitate H<sub>2</sub>O<sub>2</sub> diffusion across the OM and control its permeability.** It is often assumed that H<sub>2</sub>O<sub>2</sub> can freely cross membranes. However, several studies show that certain membranes are poorly permeable to H<sub>2</sub>O<sub>2</sub> (3, 17–19). In these membranes, permeability can be regulated by changes in membrane lipid composition or by diffusion-facilitating channel proteins. To study membrane permeability for H<sub>2</sub>O<sub>2</sub> in Gram-negative bacteria, we measured real-time H<sub>2</sub>O<sub>2</sub> influx by utilizing roGFP2 in the HpxF<sup>-</sup> background of *S. Typhimurium*. This particular strain is devoid of catalases and peroxidases (20) so that rapid detoxification of intrabacterial H<sub>2</sub>O<sub>2</sub> could be avoided and additionally so that biologically relevant concentrations of H<sub>2</sub>O<sub>2</sub> could be investigated (16). The detoxifying power of the HpxF<sup>-</sup> mutant was ~90-fold lower than that of wild-type (WT) *S. Typhimurium*, and exposure to increasing amounts of H<sub>2</sub>O<sub>2</sub> led to a dose-dependent response (see Fig. S1A to C in the supplemental material). After real-time monitoring of the H<sub>2</sub>O<sub>2</sub> influx in log-phase bacteria, we found that H<sub>2</sub>O<sub>2</sub> diffuses passively over the membrane in the initial period following H<sub>2</sub>O<sub>2</sub> exposure (Fig. 1A). However, we observed a previously unreported rapid reduction in H<sub>2</sub>O<sub>2</sub> influx coinciding with an intrabacterial redox potential of about -290 mV (Fig. 1A). To more accurately investigate the details of what we termed the “switching point,” we used the equation  $\text{Influx} = P \cdot A \cdot \Delta C$ , which defines the correlation between influx and membrane permeability for passive diffusion (3).

In this equation, *P* is the membrane permeability coefficient, *A* is the surface area of the bacterial membrane (which we assumed to be constant over short measurements), and  $\Delta C$  is the difference between the H<sub>2</sub>O<sub>2</sub> concentrations on both sides of the membrane. The influx over a variety of different  $\Delta C$  values was measured, and before the switching point, we found a linear correlation between influx ( $\mu\text{M/s}$ ) and  $\Delta C$ , which is consistent with the rules for passive diffusion (Fig. 2B and C). However, when analyzing influx after the switching point for equal  $\Delta C$  values, we found that influx was reduced to only ~8% of the influx before this point. Since the total bacterial surface area is constant throughout the experiment, this reduction can only be explained by rapid alterations in membrane permeability. A similar analysis of stationary-phase bacteria also revealed a switching point that led to a reduction in membrane permeability in which the remaining permeability was only ~3% of the permeability before the switching point (see Fig. S1D to F in the supplemental material). The change in membrane permeability was too fast to be facilitated by altered lipid composition, and on the basis of these findings, we hypothesized that at least part of the H<sub>2</sub>O<sub>2</sub> diffusion was facilitated by pores or channels in the OM. To verify that changes in the OM were driving the rapid alteration in membrane permeability, the OM was removed and the H<sub>2</sub>O<sub>2</sub> influx in spheroplasts was measured (see Fig. S1G in the supplemental material). In spheroplasts, no switching point was observed, indicating that changes to the OM were responsible for the rapid reduction of membrane permeability. Since the influx in spheroplasts was calculated to increase to ~350% of the H<sub>2</sub>O<sub>2</sub> influx in intact bacteria, we conclude that OM permeability is the rate-limiting determinant of overall membrane permeability. This is in agreement with previous findings obtained with other bacteria, where, because of lipid composition, the rate of

diffusion over the inner membrane is expected to be orders of magnitude greater than that over the OM (21).

Several OMPs form a beta-barrel in the OM and can potentially facilitate the diffusion of hydrophilic molecules across the OM (Fig. 1D) (22). To identify the OMPs responsible for H<sub>2</sub>O<sub>2</sub> diffusion, we created single deletion mutants of the four most abundant OMPs (OmpA, OmpC, OmpD, and OmpF) in HpxF<sup>-</sup> *S. Typhimurium* and calculated the H<sub>2</sub>O<sub>2</sub> influx for increasing  $\Delta C$  values before the switching point for each of the mutants (Fig. 1E). For easier comparisons, subsequent analysis of the influx throughout this study was done at a  $\Delta C$  of 45  $\mu\text{M}$  (before the switching point) and a  $\Delta C$  of 120  $\mu\text{M}$  (after the switching point). Our results indicated that OmpC predominantly facilitated H<sub>2</sub>O<sub>2</sub> diffusion before the switching point (Fig. 1E and F), whereas OmpA facilitated H<sub>2</sub>O<sub>2</sub> diffusion after the switching point (Fig. 1G). Under the conditions used in this study, OmpD and OmpF did not contribute to the diffusion of H<sub>2</sub>O<sub>2</sub> in *S. Typhimurium*. None of the OMPs completely abrogated membrane diffusion of H<sub>2</sub>O<sub>2</sub>, suggesting that low levels of H<sub>2</sub>O<sub>2</sub> diffuse freely across the membrane.

**Opening of the OmpA pore is controlled by its periplasmic domain and is dependent on oxidation-sensitive cysteines.** Our findings indicate rapid switching from the OmpC pore to the OmpA pore to facilitate H<sub>2</sub>O<sub>2</sub> influx at increasing levels of oxidative stress. Additionally, these results indicate that these pores can be rapidly closed or opened when oxidative stress is encountered. Interestingly, the OmpA protein differs from most other OMPs by having an extensive periplasmic domain (Fig. 1D). A key feature of this periplasmic domain is that it harbors two cysteines that have been shown to form an internal disulfide bond (23). Certain disulfide bonds have been found to depend on oxidative stress and can thereby function as a regulatory switch (24). To investigate the potential reversible nature of this OmpA-disulfide bond, we performed a mass spectrometry experiment that utilized stable isotope labeling by amino acids (SILAC) to compare disulfide bond formation in the *S. Typhimurium* proteome under oxidizing and normoxic conditions (Fig. 2A). We found that the disulfide bond between the only two cysteines in the periplasmic domain of OmpA occurred preferentially under oxidizing conditions (see Table S1 in the supplemental material). An additional genetic comparison found that these two cysteines are conserved in the periplasmic domain of OmpA in several Gram-negative bacteria (Fig. 2B). On the basis of this information, we hypothesized that the periplasmic domain of OmpA could function as a plug domain, while formation of the reversible disulfide bond could be the regulatory switch that controlled the conformation of the periplasmic domain and thereby the opening and closing of the OmpA pore. To investigate this concept, we first purified the WT periplasmic domain of OmpA (amino acids 198 to 350) and a mutant periplasmic domain that is unable to form an internal disulfide bond (cysteine 327 was replaced with a serine residue). These two purified proteins were subjected to oxidizing or reducing conditions (various concentrations of H<sub>2</sub>O<sub>2</sub> or dithiothreitol [DTT], respectively) and loaded onto a native acrylamide gel. We found that the WT OmpA periplasmic domain undergoes a conformational change upon oxidation, whereas the OmpA<sup>C327S</sup> mutant periplasmic domain does not change its conformation (Fig. 2C). Furthermore, we created a deletion mutant of the HpxF<sup>-</sup> strain that lacked the periplasmic domain (ompA<sup>198-350</sup> mutant) and a point mutant (ompA<sup>C327S</sup> mutant) that is unable to

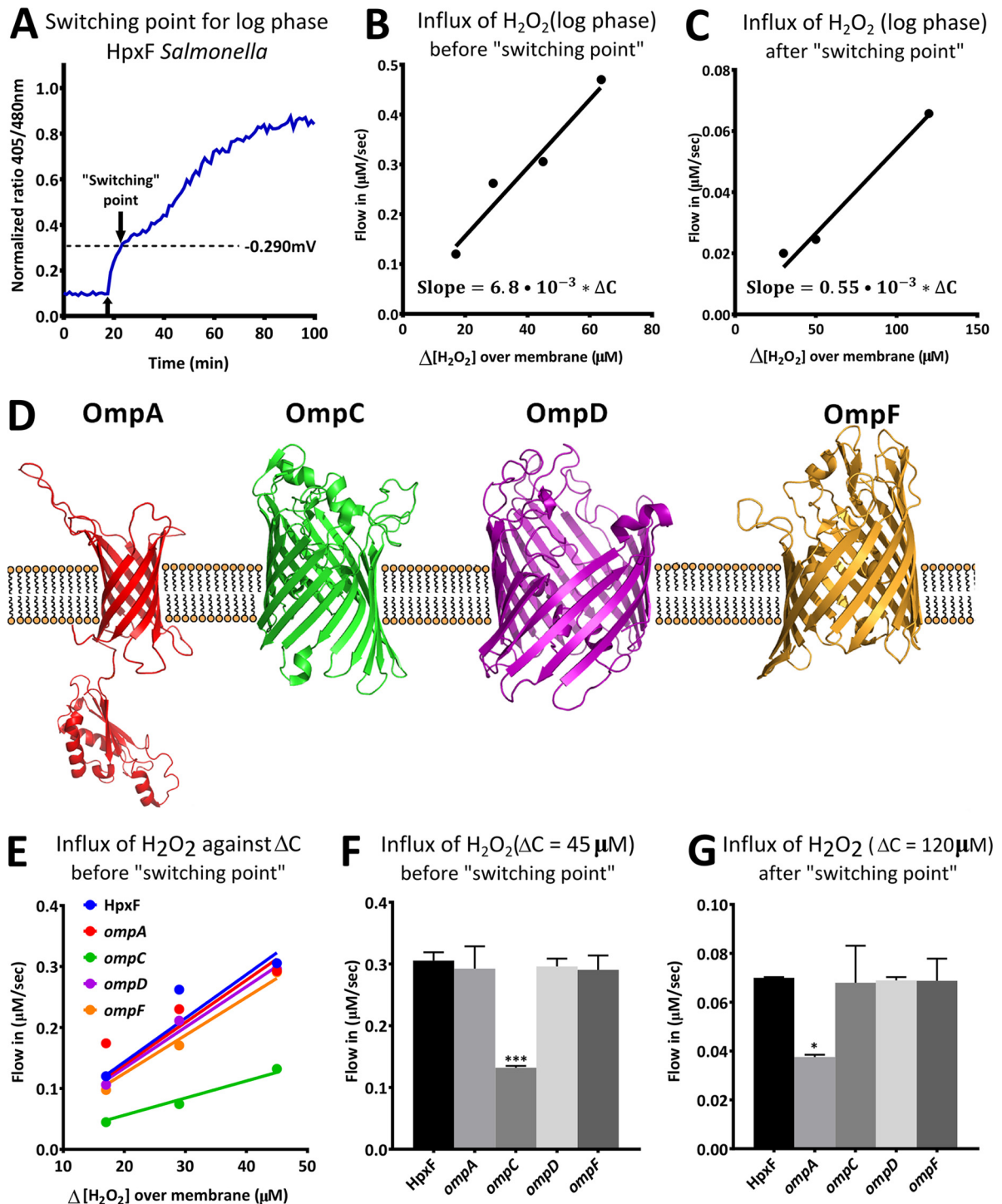


**FIG 1** *Salmonella* rapidly reduces OM permeability at the switching point. (A) Real-time analysis of changes to the intrabacterial H<sub>2</sub>O<sub>2</sub> concentration after a challenge with 150 μM H<sub>2</sub>O<sub>2</sub>. The upward-pointing arrow indicates injection of H<sub>2</sub>O<sub>2</sub>. The downward-pointing arrow indicates the moment after which the H<sub>2</sub>O<sub>2</sub> influx was suddenly reduced. We termed this moment the switching point. (B, C) Correlation between the H<sub>2</sub>O<sub>2</sub> influx across the *S. Typhimurium* membrane and ΔC before (B) and after (C) the switching point. (D) Schematic illustration of four OMPs in the OM. The protein structures of OmpA, OmpC, OmpF, and the periplasmic domain of OmpA were taken from <http://www.wwpdb.org/>. The structural prediction of OmpD was performed with the iTasser server at <http://zhanglab.cmb.med.umich.edu/I-TASSER/>. (E) For each of the single OMP deletion mutants, a correlation between the H<sub>2</sub>O<sub>2</sub> influx and ΔC was obtained before the switching point. (F, G) H<sub>2</sub>O<sub>2</sub> influx levels were obtained before and after the switching point at ΔC = 45 μM and ΔC = 120 μM, respectively. All experiments were done with mutants in the HpxF<sup>-</sup> background. Each value represents the average of four separate experiments. Error bars represent the standard deviation, and statistical significance was determined by one-way analysis of variance with comparison to the HpxF<sup>-</sup> group (\*,  $P < 0.05$ ; \*\*\*,  $P < 0.001$ ).

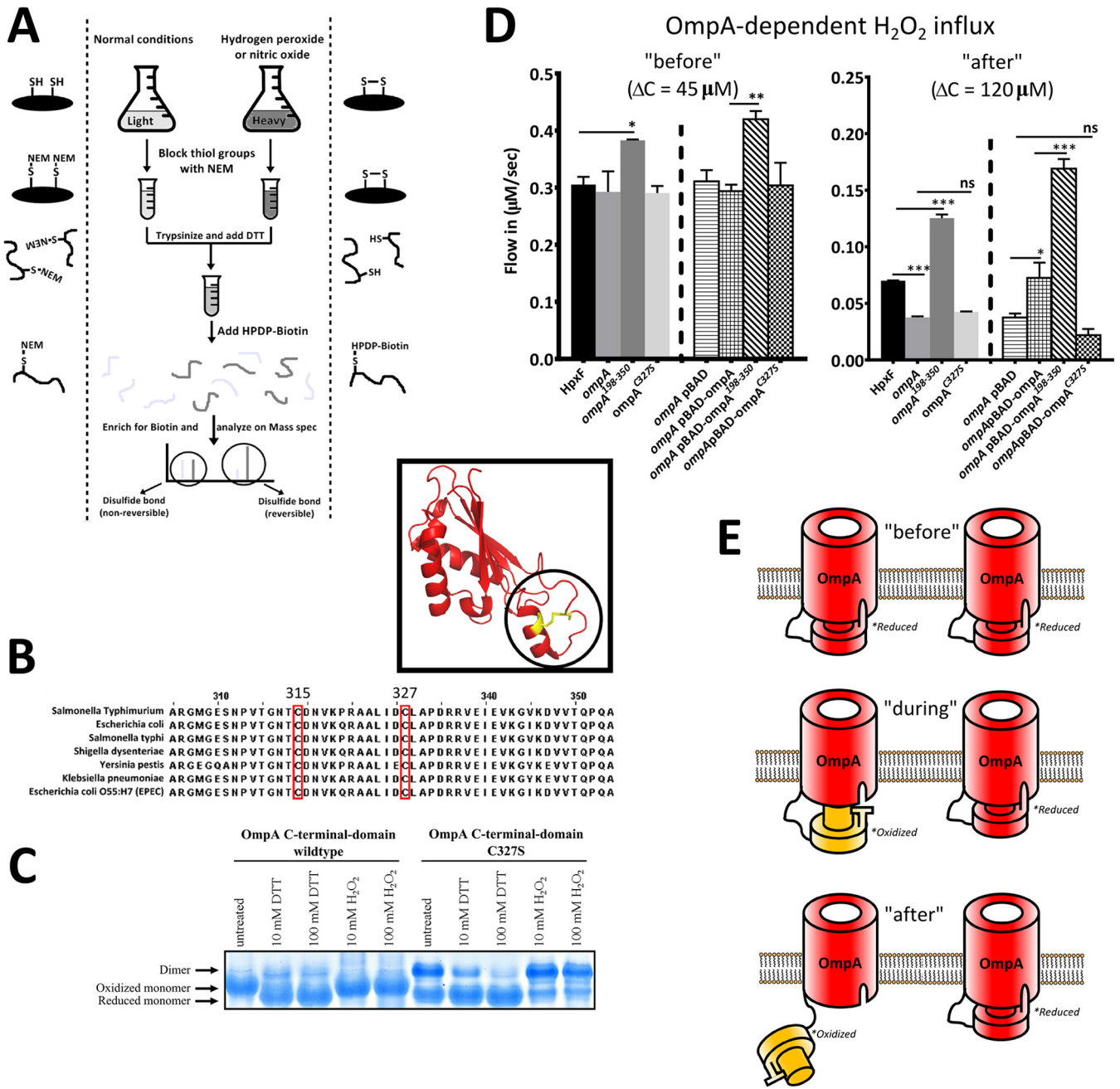
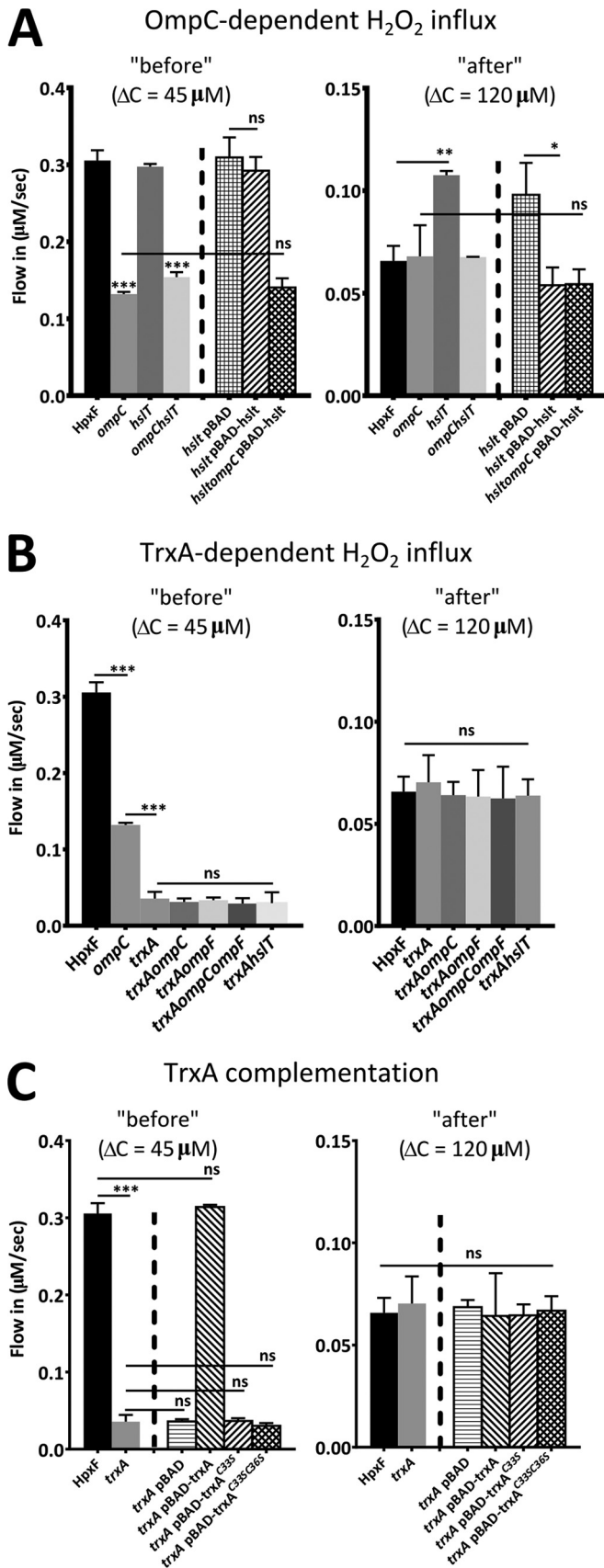


**FIG 2** Opening of the OmpA pore is regulated by its periplasmic domain. (A) SILAC mass spectrometry proteomics procedure aimed at identifying reversible disulfide bonds in the *S. Typhimurium* proteome. Bacterial cultures were grown for 5 h while their proteome was labeled with light or heavy amino acids. After exposure to 10 mM H<sub>2</sub>O<sub>2</sub> or 10 mM spermine NONOate (nitric oxide), the bacteria were lysed, the reversible disulfides were labeled with HPDP-biotin [*N*-[6-(biotinamido)hexyl]-3'-(2'-pyridyldithio)propionamide], and the peptides originating from the oxidized culture were compared to peptides originating from the control (normoxic) culture by mass spectrometry. (B) Sequence comparison shows that the two cysteines in the periplasmic domain of OmpA are widely conserved among many Gram-negative bacteria. (C) Native acrylamide gel showing the purified periplasmic domains of WT OmpA and mutant OmpA<sup>C327S</sup> after these were subjected to various concentrations of DTT or H<sub>2</sub>O<sub>2</sub>. The conformational change that is observed for the monomer under oxidizing conditions are visible only in lanes containing the WT periplasmic domain. It is worth noting that untreated purified proteins automatically get oxidized over time if no reducing agent is added. (D) The influx of H<sub>2</sub>O<sub>2</sub> was determined before and after the switching point. The H<sub>2</sub>O<sub>2</sub> influx levels before and after the switching point were determined at  $\Delta C = 45 \mu M$  and  $\Delta C = 120 \mu M$ , respectively. Before the switching point, the influx in the *ompA*<sup>188-350</sup> mutant was significantly higher than the influx in HpxF<sup>-</sup> *S. Typhimurium*. After the switching point, the influx in the *ompA* or *ompA*<sup>C327S</sup> mutant (which is unable to form the reversible disulfide bond) was lower than the influx in HpxF<sup>-</sup> *S. Typhimurium*. No significant difference was found between the *ompA* and *ompA*<sup>C327S</sup> mutant influx levels. The influx in the *ompA*<sup>188-350</sup> mutant was significantly higher than the influx in HpxF<sup>-</sup> *S. Typhimurium*. Complementation of *ompA* with the arabinose-inducible pBAD plasmid containing *ompA*, *ompA*<sup>188-350</sup>, or *ompA*<sup>C327S</sup> confirmed the results obtained with genomic mutations. All experiments were done with mutants in the HpxF<sup>-</sup> background. Each value represents the average of four separate experiments. Error bars represent the standard deviation, and statistical significance was determined by one-way analysis of variance with comparison to the HpxF<sup>-</sup> group (\*,  $P < 0.05$ ; \*\*,  $P < 0.01$ ; \*\*\*,  $P < 0.001$ ; ns, not significant). (E) Schematic representation of a proposed mechanism that leads to opening and closing of the OmpA pore by its periplasmic domain. Formation of the disulfide bond at the switching point regulates opening of the pore.



form an internal disulfide bond and measured the H<sub>2</sub>O<sub>2</sub> influx before and after the switching point (Fig. 2D). Before the switching point, when our data suggest that the OmpA pore is closed, deletion of the periplasmic domain resulted in increased H<sub>2</sub>O<sub>2</sub> influx, suggesting permanent opening of the pore. After the switching point, when our data indicate that the OmpA pore is opened, deletion of *ompA* and abrogation of disulfide bond formation in *ompA*<sup>C327S</sup> both resulted in decreased OM permeability. Under these circumstances, deletion of the periplasmic domain resulted in increased OM permeability, indicating that in WT bacteria, even after the switching point, not all OmpA pores are opened under our experimental conditions. Complementation of the *ompA* mutant with the arabinose-inducible pBAD plasmid containing *ompA*, *ompA*<sup>198-350</sup>, or *ompA*<sup>C327S</sup> confirmed the specific involvement of OmpA and its periplasmic domain in the regulation of H<sub>2</sub>O<sub>2</sub> influx after the switching point (Fig. 2D). These results support the concepts that the periplasmic domain of OmpA functions as a plug domain and that reversible disulfide bond formation in this periplasmic domain regulates the opening and closing of the pore. A schematic representation of the proposed mechanism is shown in Fig. 2E.

**The OmpC pore relies on the proteins HslT and TrxA for H<sub>2</sub>O<sub>2</sub> diffusion.** In contrast to the OmpA pore, the OmpC pore appeared to be opened before and closed after the switching point (Fig. 1E to G). Since the OmpC protein does not contain a periplasmic domain, we hypothesized that other periplasmic proteins could be involved in the regulation of the opening and closing of the OmpC pore. Previous studies have identified binding partners for OmpC and shown that in *Escherichia coli*, small heat shock protein A (IbpA) interacts with the OmpC protein (25). IbpA has also been found to be associated with the OM and the periplasm (26). IbpA is homologous to *Salmonella* protein HslT, with 98% sequence similarity. To determine whether HslT could be involved in the regulation of H<sub>2</sub>O<sub>2</sub> influx through the OmpC pore, we measured H<sub>2</sub>O<sub>2</sub> influx before and after the switching point in the *ompC* and *hslT* single deletion mutants and the *hslT ompC* double mutant (Fig. 3A). Before the switching point, when our data suggest that the OmpC pore is open, H<sub>2</sub>O<sub>2</sub> influx was lower in the *ompC* and *hslT ompC* mutants. After the switching

**FIG 3** HslT and TrxA are required for H<sub>2</sub>O<sub>2</sub> influx through the OmpC pore. (A) H<sub>2</sub>O<sub>2</sub> influx into *Salmonella*. H<sub>2</sub>O<sub>2</sub> influx levels before and after the switching point were determined at ΔC = 45 μM and ΔC = 120 μM, respectively. Before the switching point, the influx in *ompC* and *ompC hslT* mutant bacteria was significantly lower than the influx in HpxF<sup>-</sup> *S. Typhimurium*. After the switching point, the influx in *hslT* mutant bacteria was significantly greater than the influx in HpxF<sup>-</sup> *S. Typhimurium*. Complementation of *hslT* or *hslT ompC* with the arabinose-inducible pBAD plasmid containing the *hslT* gene reverted the phenotype observed in the *hslT* mutant background. (B) Influx of H<sub>2</sub>O<sub>2</sub> into *Salmonella* before and after the switching point. Deletion of *trxA* decreases H<sub>2</sub>O<sub>2</sub> influx before the switching point. Additional deletions of *ompC*, *ompF*, *ompC ompF*, and *hslT* do not further decrease H<sub>2</sub>O<sub>2</sub> influx before the switching point. (C) Complementation of *trxA* with the arabinose-inducible pBAD plasmid containing the *trxA* gene or the mutant *trxA*<sup>C335</sup> or *trxA*<sup>C335C365</sup> gene. Complementation with WT *trxA* reverts the decreased H<sub>2</sub>O<sub>2</sub> influx to WT levels; however, complementation with mutant *trxA* genes does not revert the decrease in membrane permeability. Each value represents the average of four separate experiments. All experiments were done with mutants in the HpxF<sup>-</sup> background. Error bars represent the standard deviation, and statistical significance was determined by one-way analysis of variance with comparison to the HpxF<sup>-</sup> group (\*, *P* < 0.05; \*\*, *P* < 0.01; \*\*\*, *P* < 0.001; ns, not significant).

point, when our findings suggest that the OmpC pore is closed, deletion of *hslT* increased H<sub>2</sub>O<sub>2</sub> influx. Influx was restored to WT levels in the *hslT ompC* mutant, indicating that increased influx in the absence of *hslT* was dependent on the presence of OmpC. Results from complementation of the *hslT* or *hslT ompC* mutant with the pBAD-*hslT* plasmid showed that increased membrane permeability in *hslT* after the switching point is specific for HslT and relies on the presence of OmpC (Fig. 3A). It is likely that other pores are involved in the control of H<sub>2</sub>O<sub>2</sub> diffusion, since an *hslT* deletion does not revert H<sub>2</sub>O<sub>2</sub> influx back to the influx that was measured before the switching point.

In addition to HslT, the OmpC pore has been found to interact with the oxidation-sensitive protein thioredoxin (TrxA) (27). After measuring the H<sub>2</sub>O<sub>2</sub> influx in a *trxA* mutant, we found that the H<sub>2</sub>O<sub>2</sub> influx before the switching point was dramatically lower in the mutant than in WT bacteria (Fig. 3B). After the switching point, no change in H<sub>2</sub>O<sub>2</sub> influx was observed. Deletion of *trxA* in combination with *ompC*, *ompF*, and/or *hslT*, did not result in further increased or decreased membrane permeability, suggesting that TrxA is required for H<sub>2</sub>O<sub>2</sub> diffusion through the OmpC pore (Fig. 3B). Since membrane permeability in a *trxA* mutant was lower than that in an *ompC* single mutant, we speculate that TrxA also aids other mechanisms of H<sub>2</sub>O<sub>2</sub> transport across the OM that were not investigated in this study. Several studies have found that TrxA forms an internal reversible disulfide bond similar to the reversible disulfide bond in the OmpA periplasmic domain (28). Transformation of *trxA* with pBAD plasmids containing either WT *trxA* or the *trxA*<sup>C33S</sup> or *trxA*<sup>C33SC36S</sup> mutant gene, which is defective in disulfide bond formation, showed that decreased membrane permeability could be reversed by complementation with *trxA* but not by complementation with either of the mutant *trxA* genes (Fig. 3C). These results suggest that TrxA and its reversible disulfide bond are required for H<sub>2</sub>O<sub>2</sub> diffusion prior to the switching point.

To control for differential expression of OMPs under mutant conditions, we tested the expression of OmpA in different mutants (see Fig. S2 in the supplemental material). No differences in the level of expression were observed. On the basis of these results, it is unlikely that differential expression of OMPs is the main reason for our observations.

**Experimentally increased OM permeability aids bacterial killing.** To our knowledge, this is the first report describing how Gram-negative bacteria rapidly control OM permeability by closing or opening pores in OMPs. To examine the clinical relevance of our findings, we assessed whether the survival of bacteria under oxidizing conditions was impaired by experimentally increased OM permeability. For this, we measured the survival of WT and *ompC*, *hslT*, and *ompC hslT* mutant bacteria after a challenge with 200 μM H<sub>2</sub>O<sub>2</sub> (Fig. 4A). Only the *hslT* mutant, which was found to have increased OM permeability, was attenuated for survival, while mutants with decreased OM permeability did not seem to be compromised. These results show that an inability to lower OM permeability impairs bacterial survival under oxidizing conditions.

We speculated that increasing OM permeability would increase antibiotic efficacy and allow for better bacterial killing. To test this hypothesis, we used our mutants with variable levels of OM permeability and tested the number of bacteria that survived exposure to cefotaxime. According to a recent publication, a brief interaction with bone marrow-derived macrophages (BMDM)

prior to antibiotic exposure can be used to increase the number of antibiotic-tolerant bacteria (10). We used this method and found that after a 30-min macrophage interaction, a greater subset of bacteria survived exposure to cefotaxime (Fig. 4B). Since the OmpC pore is larger than the OmpA pore and could therefore facilitate the diffusion of antibiotics, we quantified the numbers of surviving WT and *ompC*, *hslT*, and *ompC hslT* mutant *S. Typhimurium* bacteria after exposure to cefotaxime (Fig. 4C). It has been shown that ROS are not the driving force behind the phenotypic transformation into antibiotic-tolerant bacteria during macrophage interaction (10). Instead, macrophage interaction is merely used to increase the numbers of antibiotic-tolerant bacteria prior to antibiotic exposure. Importantly, the entire antibiotic exposure and the quantification of surviving bacteria took place *in vitro* without the presence of macrophages. The numbers of surviving bacteria were normalized to the numbers of bacteria at the start of the experiment, thereby controlling for differences in macrophage uptake and differences in growth/killing by macrophage-inflicted defense. Interestingly, we found that killing by cefotaxime was less effective in mutants with decreased OM permeability (*ompC* and *ompC hslT*), while antibiotic efficacy was greater in the *hslT* mutant (with increased OM permeability) than in WT bacteria (Fig. 4C). As a control, we determined the MICs of cefotaxime for WT or *hslT*, *ompC*, or *ompC hslT* mutant bacteria and found no significant differences (data not shown). Together, these results support the hypothesis that increased OM permeability increases antibiotic efficacy by killing a subset of the antibiotic-tolerant cells.

To further investigate this concept, we examined whether *S. Typhimurium* would survive cefotaxime treatment in a mouse model of infection. Previously, cefotaxime has been found to kill extracellular and intracellular bacteria equally effectively, which excludes potential differences because of differential cellular internalization of *S. Typhimurium* (29). We utilized an infection protocol similar to that described in a recent study showing that a subset of *Salmonella* bacteria survives antibiotic treatment of mice (11). We infected mice with *S. Typhimurium* and at 1 day postinfection began treating them with cefotaxime for 2 days. After antibiotic treatment, we found that mice still lost weight and carried antibiotic-tolerant bacteria in the spleen, liver, mesenteric lymph nodes (MLN), cecum, and colon (Fig. 4D and E). We detected the highest numbers of antibiotic-tolerant bacteria in MLN samples after cefotaxime treatment (Fig. 4E), similar to previous findings that reported the MLN as a reservoir of persister bacteria (11).

To test whether increased OM permeability would increase antibiotic efficacy, we infected mice with WT, *ompC* mutant (decreased OM permeability), *hslT* mutant (increased OM permeability), or *ompC hslT* mutant (decreased OM permeability) *S. Typhimurium*. A complicating factor in assessing the effect of experimentally increased OM permeability on antibiotic killing during mouse infections is the side effect that alterations in OM permeability sometimes lead to some attenuation of bacterial fitness/virulence. We first determined that, at day 1 postinfection (the commencement of antibiotic treatment), no significant differences in colonization of the cecum and colon existed between WT bacteria and any of the mutants (Fig. 4F). At day 1 postinfection, we found no significant colonization of systemic organs yet. To investigate the subset of antibiotic-tolerant bacteria, we focused on the MLN as the main reservoir after antibiotic treatment. In the untreated control group at 3 days postinfection, only the

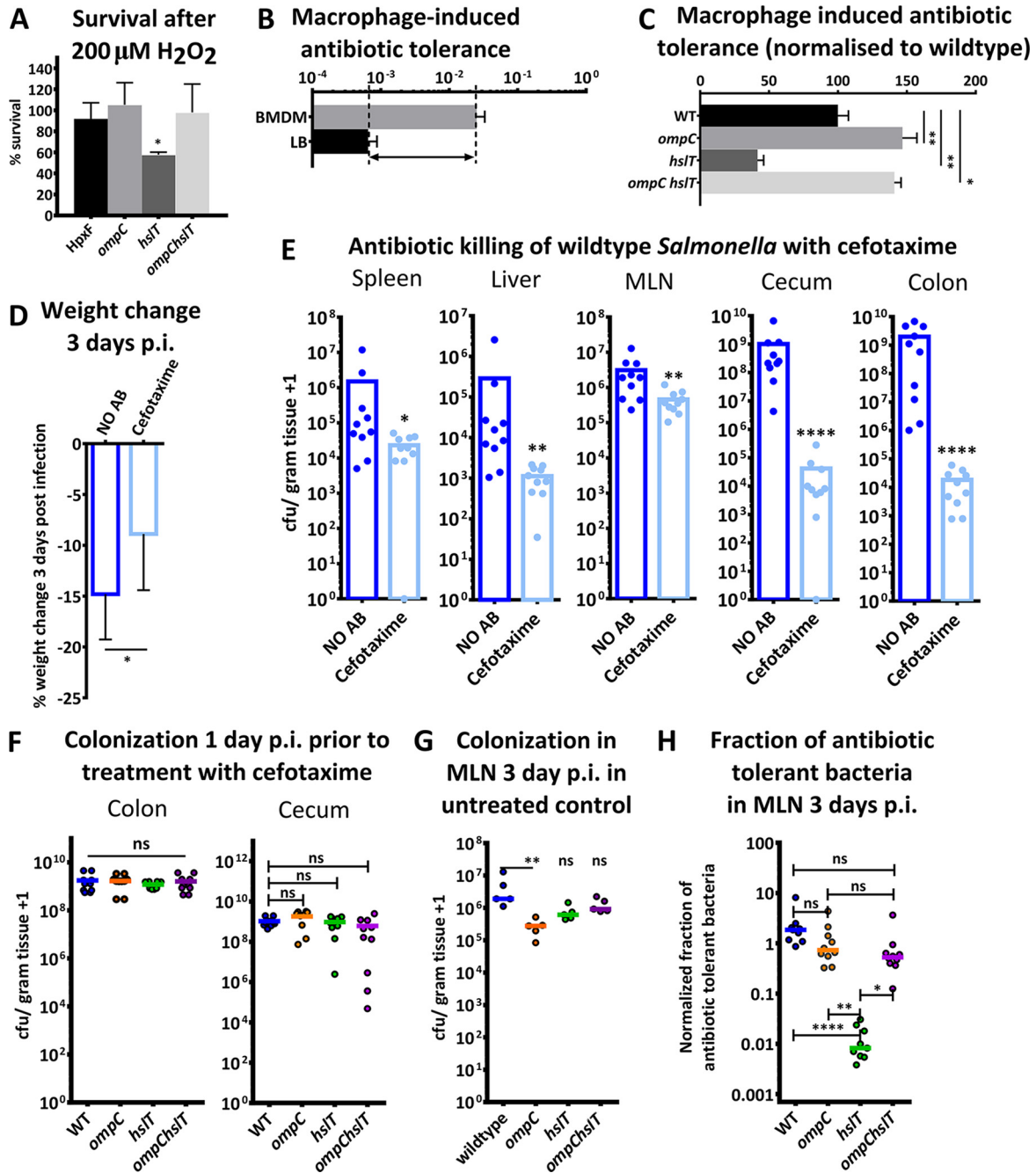


**FIG 4** Increased OM permeability increases antibiotic efficacy. (A) Percentages of *HpxF*<sup>-</sup>, *ompC*, *hslT*, and *ompC hslT* mutant bacteria that survived exposure to 200  $\mu\text{M}$   $\text{H}_2\text{O}_2$  for 2 h. These experiments were done with bacteria in the *HpxF*<sup>-</sup> background. (B) Thirty minutes after BMDM internalization, bacteria were recovered and treated with 100  $\mu\text{g}/\text{ml}$  cefotaxime for 24 h in LB. CFU counts were significantly higher on plates with *S. Typhimurium* bacteria that had interacted with BMDM. (C) Numbers of antibiotic-tolerant WT and *ompC*, *hslT*, and *ompC hslT* mutant bacteria after 24 h in LB medium supplemented with 100  $\mu\text{g}/\text{ml}$  cefotaxime. For each mutant, equal numbers of bacteria that were retrieved from BMDM were analyzed during antibiotic treatment. Antibiotic tolerance was analyzed by *Salmonella* CFU counting. Error bars represent the standard deviation, and significance was obtained by one-way analysis of variance. (D) The body weight change of mice 3 days postinfection after treatment with saline (NO AB) or cefotaxime for 2 days beginning 1 day postinfection. Body weight change is presented as a percentage of the body weight prior to infection. (E) CFU counts of *S. Typhimurium* bacteria from the spleen, liver, MLN, cecum, and colon 3 days postinfection with or without a 2-day treatment with cefotaxime. Significantly fewer bacteria were found in each organ after antibiotic treatment. Statistical significance was determined by a Mann-Whitney test. (F) CFU counts of WT and *ompC*, *hslT*, and *ompC hslT* mutant bacteria from the colons and ceca of mice at 1 day postinfection, prior to cefotaxime treatment. No significant colonization differences from WT bacteria were observed. (G) CFU counts of WT and *ompC*, *hslT*, and *ompC hslT* mutant bacteria in the MLN at 3 days postinfection without antibiotic treatment. Only *ompC* mutant bacteria showed a slightly attenuated ability to colonize the MLN. (H) Normalized fraction of bacteria that shows antibiotic tolerance in the MLN after treatment with cefotaxime. The fraction of antibiotic-tolerant bacteria after cefotaxime treatment was normalized by using the median number of the corresponding mutant bacteria that colonized the MLN of untreated mice. All experiments were done with mutants in the WT background. Statistical significance was determined by a Kruskal-Wallis test with comparison to the WT control group (\*,  $P < 0.05$ ; \*\*,  $P < 0.01$ ; \*\*\*,  $P < 0.0001$ ; ns, not significant).

*ompC* single mutant appeared to have a slightly attenuated ability to colonize the MLN (Fig. 4G). Both the *hslT* and *ompC hslT* mutants colonized the MLN to a level similar to that of the WT bacteria. In order to control for differences in the ability to colonize the MLN, the number of bacteria that survived treatment with cefotaxime was normalized to the median number of colonizing bacteria for each of the mutants (Fig. 4H). We found that cefotaxime treatment killed significantly more *hslT* mutant than WT *S. Typhimurium* bacteria in the MLN. No significant differences were observed for *ompC* or *ompC hslT* mutant bacteria, suggesting that experimentally increased OM permeability was most likely the reason for increased antibiotic efficacy. Additional analysis of WT and *ompC*, *hslT*, and *ompC hslT* mutant bacteria at 3 days postinfection without antibiotic treatment revealed that *ompC* mutant *S. Typhimurium* bacteria have an especially attenuated ability to colonize systemic organs (see Fig. S3A in the supplemental material). Despite this apparent disadvantage, greater numbers of *ompC* mutant bacteria (decreased OM permeability) than *hslT* mutant bacteria (increased OM permeability) survived in the MLN after treatment with cefotaxime (see Fig. S3B). Together, these results suggest that artificially increasing OM permeability is an effective way of increasing antibiotic efficacy.

## DISCUSSION

In this report, we reveal a novel stress response mechanism by which *Salmonella* regulates OM permeability by opening and closing specific pores. It appears that under reducing or mildly oxidizing conditions, when bacteria can grow without extensive damage to intracellular components, rapid acquisition of hydrophilic nutrients from the environment requires the wide OmpC pore. Under more oxidizing conditions, oxidative stress can damage bacteria and by limiting the influx through closure of OmpC, bacteria likely protect themselves against ROS. Our data suggest that under these circumstances, bacteria facilitate decreased diffusion over the OM through the much smaller OmpA pore. It is likely that other pores and channels are involved in H<sub>2</sub>O<sub>2</sub> diffusion, although in this study, we focused on OmpA and OmpC only.

Previous studies by another group have identified OmpD as the main porin that facilitates H<sub>2</sub>O<sub>2</sub> transport over the OM (30). Although, at first glance, these results appear to contradict our observations, substantial differences in experimental design may explain the different involvements of OMPs in H<sub>2</sub>O<sub>2</sub> transport. Most notably, different growth media were used for *in vitro* experimentation. Whereas the *Salmonella* growth conditions in our study closely mimic the conditions encountered in the intracellular environment of macrophages (31), previous data were obtained after the growth of bacteria in lysogeny broth (30). In a separate study, Kröger et al. used transcriptome sequencing analysis to show that OmpD and OmpF are severely downregulated under conditions that mimic intracellular growth, while OmpC and OmpA are upregulated (32). On the basis of these results, we conclude that growth conditions severely impact which OMPs are responsible for H<sub>2</sub>O<sub>2</sub> transport across the OM.

The structure and function of OmpA have been controversial, with some models suggesting switching between protein conformations, resulting in larger and smaller porins (33, 34). Interestingly, some reports indicate that the disulfide bond is crucial for the folding of OmpA in the larger pore conformation (35). These results provide a potential explanation for one underlying mech-

anism for our observations since abrogation of the disulfide bond leads to lower OM permeability. Alternatively, the periplasmic domain of OmpA has been shown to bind peptidoglycan, bridging peptidoglycan to the OM (36). A different binding affinity for peptidoglycan, which may be regulated by the disulfide bond, could therefore affect the stabilization of the OM and regulate permeability. A more in-depth analysis of OmpA permeability in live bacteria is required to gain full insight into the underlying mechanisms that regulate OmpA permeability.

Although this is the first report of periplasmic proteins and periplasmic protein domains controlling OM permeability for ROS, several OMPs have been reported to directly bind small periplasmic proteins, indicating that these mechanisms may be widespread among Gram-negative bacteria (25, 37, 38). In mitochondria (which are evolutionarily related to bacteria), the concept of a plug protein controlling membrane permeability has already been shown to exist (39). Although we believe our data indicate the involvement of HslT and TrxA in the regulation of OmpC permeability, we have thus far been unable to obtain conclusive evidence of direct binding among OmpC, HslT, and TrxA. It is therefore challenging to speculate on the exact mechanisms that drive closing of the OmpC pore when oxidative stress is encountered. Previously, it has been shown that OmpC has alternative states with different permeabilities (40). HslT and TrxA might influence the proportion of channels in various states and thereby regulate permeability. Real-time monitoring of membrane transport in live bacteria is required for further exploration of OM permeability-controlling mechanisms. GFP biosensors allow for this, and the use of roGFP2 in this study shows the potential of measuring real-time H<sub>2</sub>O<sub>2</sub> fluctuations to examine membrane transport in live bacteria.

Our results show compelling evidence that increasing OM permeability has great potential for limiting the number of bacteria that survive antibiotic treatment. Recently, it has been shown that macrophage-induced antibiotic tolerance is the same in *phox*<sup>-/-</sup> mutant and WT macrophages (10). Since ROS are not the driving force behind the phenotypic changes that occur because of macrophage interaction and lead to antibiotic tolerance, we did not include *phox*<sup>-/-</sup> mutant macrophages or knockout mice deficient in ROS generation. Our findings that *hslT* mutant bacteria have increased OM permeability suggest that HslT could be targeted to increase membrane permeability and thereby the bacterial killing efficacy of antibiotics.

A recent study suggests that targeting of OM permeability can be an effective strategy for increasing antibiotic efficacy (41). That study showed that treatment of Gram-negative bacteria with a combination of silver and antibiotics increases OM permeability and thereby decreases bacterial survival after antibiotic treatment (41). These results show the promise of silver as a new approach for treating bacterial infections; however, the use of silver is non-specific and would affect all commensal and symbiotic Gram-negative members of the intestinal microbiota. Recurrent problems with untreatable *Clostridium difficile* infections after harsh antibiotic regimens highlight the importance of a targeted approach to protect a balanced microbiota. The identification of naturally occurring mechanisms that control permeability allows for the design of specific antimicrobials that target these mechanisms. By targeting specific mechanisms, these antimicrobials would be more specific for pathogenic bacteria, thereby eliminating infection while maintaining a healthy, balanced microbiome.

Although we identified two OM pores that were controlled for the ability to facilitate the diffusion of  $H_2O_2$ , we specifically examined HslT as a potential target for increasing OM permeability instead of targeting the OmpA periplasmic domain. Our reasoning was that antibiotics are often bigger molecules that permeate very slowly (or not at all) through the small OmpA pore (21). Therefore, artificially increasing permeability through the bigger OmpC pore during antibiotic treatment would have a far greater effect on antibiotic killing than opening OmpA. Additionally, the OmpA pore appeared to be open under oxidative stress conditions that are encountered during infection. Thus, we expect that targeting the OmpA periplasmic domain would have only a limited effect.

It is technically difficult to separate defects in bacterial virulence resulting from altered OM permeability from differences in antibiotic tolerance during infection experiments. During *ex vivo* experiments, we were able to experimentally separate the macrophage interaction (virulence phenotype) from the experimentation that analyzed antibiotic killing of bacteria (Fig. 4C). We therefore believe that our *in vitro* data conclusively indicate that increasing OM permeability can be used to increase antibiotic efficacy. Although we attempted to control for colonization/virulence defects during *in vivo* experiments by normalizing to an untreated control (Fig. 4H), it is considerably more challenging to separate attenuation by virulence defects from differences in antibiotic killing. Our results obtained with a mouse model of infection should therefore be interpreted with caution and used as a starting point for further experimentation aimed at increasing bacterial killing by antibiotics.

In conclusion, we identified two OM pores that bacteria can control to rapidly reduce their OM permeability in response to oxidative stress. These mechanisms were critical for bacterial survival under oxidizing conditions, and our results indicate that these mechanisms could be manipulated and become potential targets for increasing antibiotic efficacy. Pores in many OMPs are probably controlled by similar mechanisms that can be targeted by new antimicrobial therapies in order to increase OM permeability and thereby enhance the antimicrobial effects of conventional antibiotics.

## MATERIALS AND METHODS

**Bacterial strains.** All experiments were done with *S. Typhimurium* strain 12023. roGFP2 was cloned from the pRSETB vector (42) into the pfpv25 vector for constitutive expression of roGFP2 and transformed into *S. Typhimurium* (16).

**Gene deletions.** Clean, nonpolar deletions in the HpxF<sup>-</sup> background and in the WT background were made by allelic exchange with the pCDV442 vector as previously described (43).

**Fluorescence measurement of fluctuations in intrabacterial redox potential.** Real-time fluctuations of the intrabacterial  $H_2O_2$  concentration were analyzed in a Tecan fluorescence plate reader with excitation at 405 and 480 nm, while emission was measured at 510 nm (16). Prior to analysis, bacteria were grown to an optical density at 600 nm (OD<sub>600</sub>) of ~1.0 in low-phosphate medium at pH 5.8 (which is used to mimic intracellular conditions). Bacteria were washed and resuspended in saline at an OD<sub>600</sub> of 2. One hundred microliters of this bacterial culture was loaded into a black, clear-bottom, 96-well plate. Bacteria were challenged with 0, 20, 40, 60, 80, 100, 150, or 200  $\mu$ M  $H_2O_2$ , and  $H_2O_2$  influx was analyzed. Background signals from nonfluorescent bacteria were obtained in the same experiment. Additionally, the signals for fully oxidized and fully reduced bacteria were obtained by adding 100 mM  $H_2O_2$  and 10 mM DTT to the bacterial culture at the start of the experiment. The 405/480-nm

ratios were normalized to the 405/480-nm ratios for maximum oxidized and reduced conditions. Each experiment was replicated at least four times. No statistical methods were used to predetermine sample size.

**Calculation of redox potential.** Calculation of the intrabacterial redox potential ( $E_{roGFP2}$ ) was done as previously described (16, 44).

**Calculation of  $H_2O_2$  influx.** To determine  $\Delta C$ , which is given by the equation  $\Delta C = C_{out} - C_{in}$ , we obtained the intrabacterial [ $H_2O_2$ ] ( $C_{in}$ ) by using the correlation between the normalized 405/480-nm ratio and the intrabacterial [ $H_2O_2$ ] that we obtained in Fig. S1C in the supplemental material. Additionally, by using  $k_{cat}$  (see Fig. S1B) and by knowing the time that has passed since the initial  $H_2O_2$  challenge ( $dt$ ), we calculated  $C_{out}$  as follows:  $C_{out} = C_{start} - (k_{cat} \cdot dt)$ .

For most of the analysis in this study, we chose to calculate the influx before the switching point at  $\Delta C = 45 \mu$ M and after the switching point at  $\Delta C = 120 \mu$ M. At these moments in our data analysis, we obtained the  $H_2O_2$  influx as follows:  $Influx = (\Delta C_{in}/dt)$ .

**Quantification of antibiotic-tolerant bacteria.** Quantification of antibiotic tolerance was done as previously described (10). In short, bacteria were grown overnight in LB medium and inoculated into fresh LB medium (1/400 dilution) containing cefotaxime (100  $\mu$ g/ml). Prior to treatment, a sample was taken and dilutions were plated to determine the inoculum size. Bacteria were incubated for 24 h at 37°C while shaking before being washed twice in phosphate-buffered saline (PBS) and plated for CFU counting. Macrophage-induced antibiotic tolerance was induced by incubation with BMDM for 30 min. After 30 min, cells were washed with PBS three times and then lysed with lysis buffer (1% Triton X-100, 0.1% SDS in PBS). Inoculum size was determined by plating the bacteria after interaction with BMDM. The inoculum was incubated in fresh LB medium containing cefotaxime (100  $\mu$ g/ml) for 24 h at 37°C while shaking before being washed twice in PBS and plated for CFU counting. The total number of antibiotic-tolerant bacteria was normalized to the inoculum size.

**Mouse infections.** Six- to 8-week-old C57BL/6 female mice were purchased from Jackson Laboratories. Twenty-four hours prior to infection, mice were given 20 mg of streptomycin sulfate (Gold Biotechnology) by oral gavage to ensure high levels of *Salmonella* gastrointestinal colonization. Mice were orally infected with  $\sim 5 \times 10^7$  CFU of streptomycin-resistant *S. Typhimurium* strain 12023 (WT or *hslT* or *ompC hslT* mutant). Since mice were infected with different bacterial strains (and mice shed infectious bacteria after infection), mice infected with different strains were kept in different cages. Beginning 24 h following infection, mice were administered either 100 mg/kg cefotaxime in  $H_2O$  (Cayman Chemical Co.) by subcutaneous injection or control  $H_2O$  subcutaneous injections twice daily for 2 days. Mice were sacrificed 3 days after *S. Typhimurium* infection, and organs were collected, weighed, homogenized, and plated on LB plates containing 100  $\mu$ g/ml streptomycin sulfate (Gold Biotechnology) for determination of numbers of *S. Typhimurium* CFU per gram of tissue. A blinded observer determined CFU counts. The animal work presented in this report was approved by the University of British Columbia Animal Care Committee (certificate number A13-0265). Results presented in this report show data from individual mice tested. The data shown are pooled data from at least two different experiments. No statistical methods were used to predetermine sample size.

## SUPPLEMENTAL MATERIAL

Supplemental material for this article may be found at <http://mbio.asm.org/lookup/suppl/doi:10.1128/mBio.01238-16/-/DCSupplemental>.

Text S1, DOCX file, 0.04 MB.

Figure S1, TIF file, 0.7 MB.

Figure S2, TIF file, 1.6 MB.

Figure S3, TIF file, 1 MB.

Table S1, DOCX file, 0.02 MB.

## ACKNOWLEDGMENTS

This work was supported by operating grants from the Canadian Institutes of Health Research (CIHR). B.B.F. is the University of British Co-

lumbia Peter Wall Distinguished Professor. No competing interests exist for this work.

We sincerely thank James Remington of the University of Oregon for providing the original pRSETB roGFP2 construct and Laurent Aussel of the Institut de Microbiologie de la Méditerranée for providing the HpxF-*Salmonella* strain.

## FUNDING INFORMATION

This work, including the efforts of B. Brett Finlay, was funded by Canadian Institutes for Health Research (MOP-133561).

## REFERENCES

- Delcour AH. 2009. Outer membrane permeability and antibiotic resistance. *Biochim Biophys Acta* 1794:808–816. <http://dx.doi.org/10.1016/j.bbapap.2008.11.005>.
- Imlay JA. 2013. The molecular mechanisms and physiological consequences of oxidative stress: lessons from a model bacterium. *Nat Rev Microbiol* 11:443–454. <http://dx.doi.org/10.1038/nrmicro3032>.
- Seaver LC, Imlay JA. 2001. Hydrogen peroxide fluxes and compartmentalization inside growing *Escherichia coli*. *J Bacteriol* 183:7182–7189. <http://dx.doi.org/10.1128/JB.183.24.7182-7189.2001>.
- Mahendran KR, Kreir M, Weingart H, Fertig N, Winterhalter M. 2010. Permeation of antibiotics through *Escherichia coli* OmpF and OmpC porins: screening for influx on a single-molecule level. *J Biomol Screen* 15:302–307. <http://dx.doi.org/10.1177/1087057109357791>.
- Masi M, Pagès JM. 2013. Structure, function and regulation of outer membrane proteins involved in drug transport in Enterobacteriaceae: the OmpF/C-TolC case. *Open Microbiol J* 7:22–33. <http://dx.doi.org/10.2174/1874285801307010022>.
- Lavigne JP, Sotto A, Nicolas-Chanoine MH, Bouziges N, Bourg G, Davin-Regli A, Pagès JM. 2012. Membrane permeability, a pivotal function involved in antibiotic resistance and virulence in *Enterobacter aerogenes* clinical isolates. *Clin Microbiol Infect* 18:539–545. <http://dx.doi.org/10.1111/j.1469-0691.2011.03607.x>.
- Bumann D. 2015. Heterogeneous host-pathogen encounters: act locally, think globally. *Cell Host Microbe* 17:13–19. <http://dx.doi.org/10.1016/j.chom.2014.12.006>.
- Macfarlane EL, Kwasnicka A, Hancock RE. 2000. Role of *Pseudomonas aeruginosa* PhoP-phoQ in resistance to antimicrobial cationic peptides and aminoglycosides. *Microbiology* 146:2543–2554. <http://dx.doi.org/10.1099/00221287-146-10-2543>.
- Schmidt NW, Deshayes S, Hawker S, Blacker A, Kasko AM, Wong GC. 2014. Engineering persister-specific antibiotics with synergistic antimicrobial functions. *ACS Nano* 8:8786–8793. <http://dx.doi.org/10.1021/nm502201a>.
- Helaine S, Cheverton AM, Watson KG, Faure LM, Matthews SA, Holden DW. 2014. Internalization of *Salmonella* by macrophages induces formation of nonreplicating persisters. *Science* 343:204–208. <http://dx.doi.org/10.1126/science.1244705>.
- Kaiser P, Regoes RR, Dolowschiak T, Wotzka SY, Lengefeld J, Slack E, Grant AJ, Ackermann M, Hardt WD. 2014. Cecum lymph node dendritic cells harbor slow-growing bacteria phenotypically tolerant to antibiotic treatment. *PLoS Biol* 12:e1001793. <http://dx.doi.org/10.1371/journal.pbio.1001793>.
- Diard M, Sellin ME, Dolowschiak T, Arnoldini M, Ackermann M, Hardt WD. 2014. Antibiotic treatment selects for cooperative virulence of *Salmonella* Typhimurium. *Curr Biol* 24:2000–2005. <http://dx.doi.org/10.1016/j.cub.2014.07.028>.
- Claudi B, Spröte P, Chirkova A, Personnic N, Zankl J, Schürmann N, Schmidt A, Bumann D. 2014. Phenotypic variation of *Salmonella* in host tissues delays eradication by antimicrobial chemotherapy. *Cell* 158:722–733. <http://dx.doi.org/10.1016/j.cell.2014.06.045>.
- Hurdle JG, O'Neill AJ, Chopra I, Lee RE. 2011. Targeting bacterial membrane function: an underexploited mechanism for treating persistent infections. *Nat Rev Microbiol* 9:62–75. <http://dx.doi.org/10.1038/nrmicro2474>.
- van der Heijden J, Vogt SL, Reynolds LA, Peña-Díaz J, Tupin A, Aussel L, Finlay BB. 2016. Exploring the redox balance inside Gram-negative bacteria with redox-sensitive GFP. *Free Radic Biol Med* 91:34–44. <http://dx.doi.org/10.1016/j.freeradbiomed.2015.11.029>.
- van der Heijden J, Bosman ES, Reynolds LA, Finlay BB. 2015. Direct measurement of oxidative and nitrosative stress dynamics in *Salmonella* inside macrophages. *Proc Natl Acad Sci U S A* 112:560–565. <http://dx.doi.org/10.1073/pnas.1414569112>.
- Antunes F, Cadenas E. 2000. Estimation of H<sub>2</sub>O<sub>2</sub> gradients across biomembranes. *FEBS Lett* 475:121–126. [http://dx.doi.org/10.1016/S0014-5793\(00\)01638-0](http://dx.doi.org/10.1016/S0014-5793(00)01638-0).
- Sousa-Lopes A, Antunes F, Cyrne L, Marinho HS. 2004. Decreased cellular permeability to H<sub>2</sub>O<sub>2</sub> protects *Saccharomyces cerevisiae* cells in stationary phase against oxidative stress. *FEBS Lett* 578:152–156. <http://dx.doi.org/10.1016/j.febslet.2004.10.090>.
- Bienert GP, Schjoerring JK, Jahn TP. 2006. Membrane transport of hydrogen peroxide. *Biochim Biophys Acta* 1758:994–1003. <http://dx.doi.org/10.1016/j.bbamem.2006.02.015>.
- Hébrard M, Viala JP, Méresse S, Barras F, Aussel L. 2009. Redundant hydrogen peroxide scavengers contribute to *Salmonella* virulence and oxidative stress resistance. *J Bacteriol* 191:4605–4614. <http://dx.doi.org/10.1128/JB.00144-09>.
- Sugawara E, Nikaido H. 2012. OmpA is the principal nonspecific slow porin of *Acinetobacter baumannii*. *J Bacteriol* 194:4089–4096. <http://dx.doi.org/10.1128/JB.00435-12>.
- Wiener MC, Horanyi PS. 2011. How hydrophobic molecules traverse the outer membranes of Gram-negative bacteria. *Proc Natl Acad Sci U S A* 108:10929–10930. <http://dx.doi.org/10.1073/pnas.1106927108>.
- Lu S, Fan SB, Yang B, Li YX, Meng JM, Wu L, Li P, Zhang K, Zhang MJ, Fu Y, Luo J, Sun RX, He SM, Dong MQ. 2015. Mapping native disulfide bonds at a proteome scale. *Nat Methods* 12:329–331. <http://dx.doi.org/10.1038/nmeth.3283>.
- Hillion M, Antelmann H. 2015. Thiol-based redox switches in prokaryotes. *Biol Chem* 396:415–444. <http://dx.doi.org/10.1515/hsz-2015-0102>.
- Butland G, Peregrín-Alvarez JM, Li J, Yang W, Yang X, Canadien V, Starostine A, Richards D, Beattie B, Krogan N, Davey M, Parkinson J, Greenblatt J, Emili A. 2005. Interaction network containing conserved and essential protein complexes in *Escherichia coli*. *Nature* 433:531–537. <http://dx.doi.org/10.1038/nature03239>.
- Kuczyńska-Wiśnik D, Kedzierska S, Matuszewska E, Lund P, Taylor A, Lipińska B, Laskowska E. 2002. The *Escherichia coli* small heat-shock proteins IbpA and IbpB prevent the aggregation of endogenous proteins denatured *in vivo* during extreme heat shock. *Microbiology* 148:1757–1765. <http://dx.doi.org/10.1099/00221287-148-6-1757>.
- Kumar JK, Tabor S, Richardson CC. 2004. Proteomic analysis of thioredoxin-targeted proteins in *Escherichia coli*. *Proc Natl Acad Sci U S A* 101:3759–3764. <http://dx.doi.org/10.1073/pnas.0308701101>.
- Arner ES, Holmgren A. 2000. Physiological functions of thioredoxin and thioredoxin reductase. *Eur J Biochem* 267:6102–6109. <http://dx.doi.org/10.1046/j.1432-1327.2000.01701.x>.
- Ekinci B, Coban AY, Birinci A, Durupinar B, Erturk M. 2002. In vitro effects of cefotaxime and ceftriaxone on *Salmonella typhi* within human monocyte-derived macrophages. *Clin Microbiol Infect* 8:810–813. <http://dx.doi.org/10.1046/j.1469-0691.2002.00457.x>.
- Calderón IL, Morales E, Caro NJ, Chahúan CA, Collao B, Gil F, Villarreal JM, Ipinza F, Mora GC, Saavedra CP. 2011. Response regulator ArcA of *Salmonella enterica* serovar Typhimurium downregulates expression of OmpD, a porin facilitating uptake of hydrogen peroxide. *Res Microbiol* 162:214–222. <http://dx.doi.org/10.1016/j.resmic.2010.11.001>.
- Coombs BK, Brown NF, Valdez Y, Brumell JH, Finlay BB. 2004. Expression and secretion of *Salmonella* pathogenicity island-2 virulence genes in response to acidification exhibit differential requirements of a functional type III secretion apparatus and SsaL. *J Biol Chem* 279:49804–49815. <http://dx.doi.org/10.1074/jbc.M404299200>.
- Kröger C, Colgan A, Srikumar S, Händler K, Sivasankaran SK, Hammarlöf DL, Canals R, Grissom JE, Conway T, Hokamp K, Hinton JC. 2013. An infection-relevant transcriptomic compendium for *Salmonella enterica* serovar Typhimurium. *Cell Host Microbe* 14:683–695. <http://dx.doi.org/10.1016/j.chom.2013.11.010>.
- Smith SG, Mahon V, Lambert MA, Fagan RP. 2007. A molecular Swiss army knife: OmpA structure, function and expression. *FEMS Microbiol Lett* 273:1–11. <http://dx.doi.org/10.1111/j.1574-6968.2007.00778.x>.
- Reusch RN. 2012. Insights into the structure and assembly of *Escherichia coli* outer membrane protein A. *FEBS J* 279:894–909. <http://dx.doi.org/10.1111/j.1742-4658.2012.08484.x>.
- Negoda A, Negoda E, Reusch RN. 2010. Resolving the native conforma-

- tion of *Escherichia coli* OmpA. FEBS J 277:4427–4437. <http://dx.doi.org/10.1111/j.1742-4658.2010.07823.x>.
36. Park JS, Lee WC, Yeo KJ, Ryu KS, Kumarasiri M, Hesek D, Lee M, Mobashery S, Song JH, Kim SI, Lee JC, Cheong C, Jeon YH, Kim HY. 2012. Mechanism of anchoring of OmpA protein to the cell wall peptidoglycan of the Gram-negative bacterial outer membrane. FASEB J 26: 219–228. <http://dx.doi.org/10.1096/fj.11-188425>.
  37. Pilonieta MC, Erickson KD, Ernst RK, Detweiler CS. 2009. A protein important for antimicrobial peptide resistance, YdeI/OmdA, is in the periplasm and interacts with OmpD/NmpC. J Bacteriol 191:7243–7252. <http://dx.doi.org/10.1128/JB.00688-09>.
  38. Arifuzzaman M, Maeda M, Itoh A, Nishikata K, Takita C, Saito R, Ara T, Nakahigashi K, Huang HC, Hirai A, Tsuzuki K, Nakamura S, Altaf-Ul-Amin M, Oshima T, Baba T, Yamamoto N, Kawamura T, Ioka-Nakamichi T, Kitagawa M, Tomita M. 2006. Large-scale identification of protein-protein interaction of *Escherichia coli* K-12. Genome Res 16:686–691. <http://dx.doi.org/10.1101/gr.4527806>.
  39. Rostovtseva TK, Sheldon KL, Hassanzadeh E, Monge C, Saks V, Bezrukov SM, Sackett DL. 2008. Tubulin binding blocks mitochondrial voltage-dependent anion channel and regulates respiration. Proc Natl Acad Sci U S A 105:18746–18751. <http://dx.doi.org/10.1073/pnas.0806303105>.
  40. Biró I, Pezeshki S, Weingart H, Winterhalter M, Kleinekathöfer U. 2010. Comparing the temperature-dependent conductance of the two structurally similar *E. coli* porins OmpC and OmpF. Biophys J 98: 1830–1839. <http://dx.doi.org/10.1016/j.bpj.2010.01.026>.
  41. Morones-Ramirez JR, Winkler JA, Spina CS, Collins JJ. 2013. Silver enhances antibiotic activity against Gram-negative bacteria. Sci Transl Med 5:190ra81. <http://dx.doi.org/10.1126/scitranslmed.3006276>.
  42. Hanson GT, Aggeler R, Oglesbee D, Cannon M, Capaldi RA, Tsien RY, Remington SJ. 2004. Investigating mitochondrial redox potential with redox-sensitive green fluorescent protein indicators. J Biol Chem 279: 13044–13053. <http://dx.doi.org/10.1074/jbc.M312846200>.
  43. Edwards RA, Keller LH, Schifferli DM. 1998. Improved allelic exchange vectors and their use to analyze 987P fimbria gene expression. Gene 207: 149–157. [http://dx.doi.org/10.1016/S0378-1119\(97\)00619-7](http://dx.doi.org/10.1016/S0378-1119(97)00619-7).
  44. van der Heijden J, Finlay BB. 2015. *In vitro* real-time measurement of the intra-bacterial redox potential. Bio Protoc 5:e1579. <http://www.bio-protocol.org/e1579>.